JKAS
Journal of the Korean Astronomical Society
http://jkas.kas.org
eISSN: 2288-890X · pISSN: 1225-4614
JKAS (2024), **57**, 2, 145–154
doi: 10.5303/JKAS.2024.57.2.145

Asteroseismic Searching for Environmental Influence in Star Clusters Observed by *Kepler*/*K2*

Yun-A Jo and Heon-Young Chang*

Department of Astronomy, Kyungpook National University, Daegu 41566, Republic of Korea
*Corresponding Author: H.-Y. Chang, hyc@knu.ac.kr

Received April 29, 2024; Accepted August 15, 2024; Published August 29, 2024

Abstract

In this paper, we investigate asteroseismic scaling-relations of evolved stars in star clusters observed by *Kepler*/*K2*, aiming to address the issue of whether observed stellar oscillations are influenced by environmental factors, as there are interesting phenomena relating to the stellar pulsations observed in star clusters. Specifically, we compare statistical properties of distributions including $\Delta\nu$, $\nu_{\rm max}$, $H_{\rm Gauss}$, $\delta\nu_{\rm env}$, and $\delta\nu_{02}$ derived from red giant branch (RGB) and red clump (RC) stars in two pairs of star clusters: NGC 2682 - NGC 6819 and NGC 1817 - NGC 6811. We have found that the slopes of relations between $\nu_{\rm max}$ and $\Delta\nu$ and between $H_{\rm Gauss}$ and $\nu_{\rm max}$ associated with RC stars in the more compact star clusters, NGC 2682 and NGC 1817, are in common less steep compared with those for NGC 6819 and NGC 6811. It is also found that the slopes of the relation between $\delta\nu_{\rm env}$ and $\nu_{\rm max}$ from RC stars in the more compact star clusters are in common steeper compared with those for the others. For the relation between $\delta\nu_{02}$ and $\Delta\nu$ obtained from RGB stars, the slope resulting from NGC 2682 and NGC 6819 is indistinguishable. The Kolmogorov–Smirnov tests conducted on RC stars in the pairs of NGC 2682 and NGC 6819, as well as NGC 1817 and NGC 6811, indicate that all the seismic quantities considered in this paper are drawn from different distributions. We conclude, therefore, that the properties of star clusters should be considered when asteroseismic data obtained from stars within star clusters are interpreted.

Keywords: asteroseismology — methods: data analysis — stars: fundamental parameters

1. Introduction

There are interesting phenomena relating to the stellar pulsations observed in star clusters. In particular, there are pulsators outside instability strips in the Hertzsprung-Russell (HR) diagram where no pulsation could be predicted using standard stellar models. For instance, Mowlavi et al. (2016) reported pulsating stars in the field of view of the relatively young open cluster NGC 3766, located in the vast star-forming region known as the Carina molecular cloud. To gain a better understanding of the relation between the environment and stellar pulsation process, therefore, effort should be devoted to studying pulsating stars in the context of asteroseismology.

Asteroseismology enhances our knowledge of the internal structure and dynamics of the Sun-like stars by exploring the stellar oscillation modes appearing as peaks in the observed stellar power spectrum (Hekker et al. 2009; Basu et al. 2011; Chaplin & Miglio 2013; Coelho et al. 2015; Anders et al. 2017; Yu et al. 2018; Howell et al. 2022; Zhou et al. 2024a). The frequencies of solar-like oscillations for modes with high radial order n and low spherical degree l are well approximated by the following asymptotic relation (Tassoul 1980; Gough 1986):

$$\nu_{n,l} \simeq \Delta\nu \left(n + \frac{l}{2} + \epsilon \right) - \delta\nu_{0l}, \tag{1}$$

where the frequency difference $\Delta\nu$ is the large frequency separation between modes of the same degree with consecutive radial order, ϵ is a phase shift near the stellar surface, and $\delta\nu_{0l}$ is the small frequency separation of non-radial modes with respect to radial modes within the same radial order. In particular, average frequency separations allow us to seismically deduce an overview of stars even without requiring thorough asteroseismic analysis. Note that $\Delta\nu$ is inversely proportional to the sound-travel time between the center and surface of a star, corresponding to the reciprocal of its dynamical or acoustic time-scale, specified as

$$\Delta\nu \propto \bar{\rho}^{1/2} \propto \left(\frac{M}{\rm M_\odot} \right)^{1/2} \left(\frac{R}{\rm R_\odot} \right)^{-3/2}, \tag{2}$$

where $\bar{\rho}$ is the mean density of a star, M is its mass, and R is its radius. The small frequency separation $\delta\nu_{02}$ between modes of $l = 0$ and $l = 2$ for a given radial order is used to infer

the gradient of the mean molecular weight in the core, which decreases as the star ages (Christensen-Dalsgaard 1988).

With the emergence of precise and accurate asteroseismic measurements provided by space missions, such as MOST (Walker et al. 2003), CoRoT (Baglin et al. 2006; Michel et al. 2008), *Kepler* (Borucki et al. 2010; Koch et al. 2010), and TESS (Ricker et al. 2015), asteroseismology allows one to exploit empirical scaling relations based on the global asteroseismic parameters. In this case, instead of a series of distinct peaks, the observed stellar power spectrum is described as a whole by the stellar oscillation power excess centered at $\nu_{\rm max}$ with the width of the Gaussian envelope being $\delta\nu_{\rm env}$ and the background noise originating by various features in the stellar atmosphere (Harvey 1985; Harvey et al. 1993; Karoff 2008; Mathur et al. 2011).

Supposed that $\nu_{\rm max}$ is proportional to the cut-off frequency $\nu_{\rm c}$ above which total reflection cannot occur at the star surface, the observed $\nu_{\rm max}$ for an isothermal atmosphere can be expressed as follows:

$$\begin{aligned}\nu_{\rm max} &\propto \frac{c_{\rm s}}{H_{\rm p}} \propto \frac{g}{\sqrt{T_{\rm eff}}} \\ &\propto \left(\frac{M}{\rm M_\odot}\right)\left(\frac{R}{\rm R_\odot}\right)^{-2}\left(\frac{T_{\rm eff}}{\rm T_{eff,\odot}}\right)^{-1/2},\end{aligned} \tag{3}$$

where $c_{\rm s}$ is the speed of sound, $H_{\rm p}$ is the scale height of pressure, g is the surface gravity, and $T_{\rm eff}$ is the effective temperature (Brown et al. 1991; Kjeldsen & Bedding 1995; Belkacem et al. 2011). Although the theoretical basis for $\delta\nu_{\rm env}$ is not as solid as that of $\nu_{\rm max}$, $\delta\nu_{\rm env}$ is considered to be a measure of the efficiency in the excitation and damping of solar-like oscillations (Mosser et al. 2012). By scaling $\Delta\nu$ and $\nu_{\rm max}$ of stars to those of the Sun, one obtains an estimate of stellar masses and radii within an uncertainty of $\sim$4% and 16% for MS stars and red giants, respectively, as (Silva Aguirre et al. 2011, 2018; Miglio et al. 2012; Sharma et al. 2016; Pinsonneault et al. 2018; Brogaard et al. 2018; Kallinger et al. 2018; Bellinger 2020; Zhou et al. 2024b):

$$\frac{M}{\rm M_\odot} \simeq \left(\frac{\nu_{\rm max}}{\nu_{\rm max,\odot}}\right)^{3}\left(\frac{\Delta\nu}{\Delta\nu_\odot}\right)^{-4}\left(\frac{T_{\rm eff}}{\rm T_{eff,\odot}}\right)^{3/2}, \tag{4}$$

$$\frac{R}{\rm R_\odot} \simeq \left(\frac{\nu_{\rm max}}{\nu_{\rm max,\odot}}\right)\left(\frac{\Delta\nu}{\Delta\nu_\odot}\right)^{-2}\left(\frac{T_{\rm eff}}{\rm T_{eff,\odot}}\right)^{1/2}. \tag{5}$$

The solar values for $\Delta\nu_\odot$ and $\nu_{\rm max,\odot}$ are typically 135.1 μHz and 3090 μHz, respectively (Chaplin et al. 2014).

Mosser et al. (2010) analyzed 1800 evolved field stars observed by CoRoT, launched on 2006 December 27, and investigated asteroseismic parameters. Having done that, they were able to compare the properties of red giants in two opposite fields of the Galaxy. By comparing the stars observed in two different regions, they have found that the stellar asteroseismic properties are globally similar, but that the characteristics are different for red-clump giant stars. Miglio et al. (2013) carried out a similar study. More recently, Anders et al. (2017) attempted to examine the correlation between asteroseismic ages for 606 red giant stars and chemical abundance patterns of field stars over a broad radial range of the Milky Way disc. Since stars within a star cluster form from the gas cloud at almost the same time, comparing stars within clusters is expected to allow for a more consistent and clear analysis of the influence of environmental factors. There are many studies on solar-like oscillations in the open clusters observed by *Kepler*/*K2*, such as NGC 6791, NGC 6819, NGC 6811. However, they took advantage of cluster stars sharing common properties to focus on the mass effect by assuming that other parameters make no distinct differences (e.g., Abedigamba et al. 2016; Arentoft et al. 2017; Corsaro et al. 2017).

In this paper, we explore scaling relations to speculate whether observed solar-like oscillations are influenced by the environment. To do so, we analyze the asteroseismic data of evolved stars in star clusters observed by *Kepler*/*K2*, and carefully compare their statistical properties. As the dependence of asteroseismic relations on the stellar mass is well established (Hekker et al. 2011; Stello et al. 2011; Corsaro et al. 2017), we need to focus our attention on stars of similar mass to avoid confusion between mass effects and environmental effects. For this purpose, we exclusively study giant stars in star clusters of similar ages in the current analysis. This can be illustrated in the sense that the mass of the stars at the turn-off point is a well-determined function of the age of the star cluster (Carroll & Ostlie 2017). One advantage of pursuing this approach is that we may control the stellar mass without the need for deriving the individual mass of the star with scaling relations, which may inevitably involve some systematic errors mentioned above. Based on a series of selection criteria discussed below, we end up with two pairs of star clusters: NGC 2682 - NGC 6819 and NGC 1817 - NGC 6811. We attempt to statistically search for a clue of any environmental influence on $\Delta\nu$, $\nu_{\rm max}$, the height of the power spectrum at $\nu_{\rm max}$, and $\delta\nu_{\rm env}$, by examining whether red giant branch (RGB) stars and red clump (RC) stars in the two pairs of the star clusters consistently come to the same results. In addition, we also carry out our investigation with the relation between $\nu_{\rm max}$ and $\delta\nu_{02}$ for the pair NGC 2682 - NGC 6819.

This paper is organized as follows. We briefly describe the data being analyzed for the present paper and procedure of power-spectrum fitting we have carried out in Section 2. We present and discuss asteroseismic parameters obtained by analyzing the evolved stars in the four star clusters observed by the *Kepler*/*K2* missions in Section 3. Finally, we summarize and conclude in Section 4.

2. Data and Power Spectrum

For the current analysis, we consider oscillating members of star clusters, with $\nu_{\rm max}$ in the range of $30\,\mu{\rm Hz} < \nu_{\rm max} < 220\,\mu{\rm Hz}$, observed by the *Kepler*/*K2* missions, as we focus our attention on giant stars. We exclude subgiants and MS stars with $\nu_{\rm max} \gtrsim 220\,\mu$Hz. Furthermore, we exclude giant stars with $\nu_{\rm max} \lesssim 30\,\mu$Hz (Li et al. 2022). The NASA *Kepler* space telescope was to monitor approximately 150,000 stars in a field of view of 115 square degrees located in the constellation of Cygnus (Borucki et al. 2010; Koch et al. 2010). *Kepler*

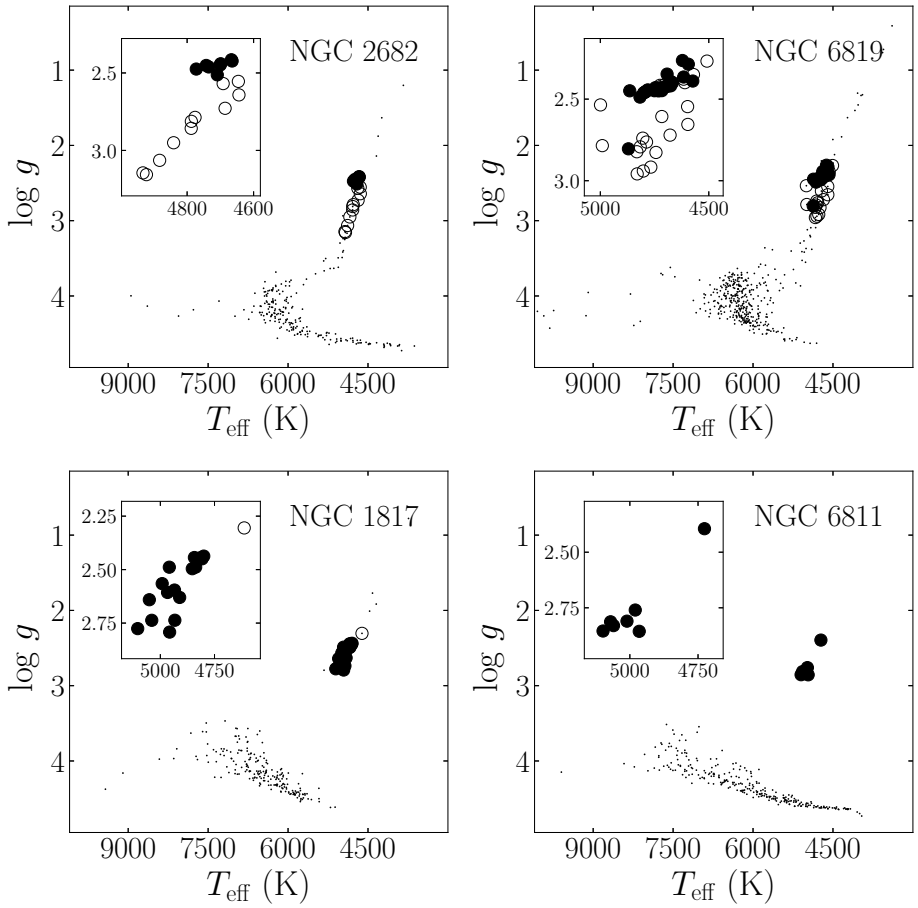

Figure 1. Kiel diagrams of the star clusters indicated in the top right. Dots are all the stars observed by the *Kepler*/*K2* missions. Open and filled circles represent RGB and RC stars, respectively, providing seismic parameters for the present analysis.

successfully made scientific observations for 17 quarters, each lasting three months. Thus, it is possible to form a single consistent time-series over multiple quarters spanning up to approximately four years. Following the loss of two reaction wheels required to maintain the pointing stability, the mission was renamed *K2*. Due to the gradual drift of its field of view across the sky (Howell et al. 2014), *K2* observes a series of independent target fields in the ecliptic plane[1] for durations of approximately 75 days, respectively.

The original *Kepler* field of view involves four open clusters: NGC 6791, NGC 6819, NGC 6811, and NGC 6866. Additionally, there were 29 star clusters, including two young stellar-associations, in the *K2* campaign fields. Because we focus our attention on oscillating evolved stars, we first choose star clusters older than 10^9 years in which evolved stars with a mass of $\sim 1\,M_\odot$ are present. This criterion is selected because it is challenging to detect oscillating evolved stars in star clusters younger than 10^9 years (Iben 1967; Sackmann et al. 1993; Schröder & Smith 2008). Among the 16 star clusters meeting this criterion, we further select star clusters comprising member stars whose light curves are available with long-cadence mode, with data points sampled every 29.4244 minutes. As a result, we have seven star clusters: NGC 6791, NGC 2682 (M67), NGC 6819, NGC 1817, NGC 6811, NGC 6121 (M4), and NGC 6774. However, NGC 6774 has been eventually excluded as the signal-to-noise ratio of the stellar power spectrum is insufficient in general. That is, only one power spectrum among 11 candidates was suitable for a fitting procedure. As we are to create pairs of star clusters with similar ages, we determine to dismiss globular cluster NGC 6121 and one of the oldest open cluster NGC 6791, which are 12.59 and 7.23 billion years old, respectively (Sharina et al. 2018; Dias et al. 2021). Consequently, we are able to form two pairs of star clusters for comparison: NGC 2682 - NGC 6819 and NGC 1817 - NGC 6811.

In Figure 1, we show Kiel diagrams of the four star clusters considered in this work. The dots are stars observed by the *Kepler*/*K2* missions. The hydrogen-shell-burning RGB stars and core-helium-burning RC stars successfully providing seismic parameters for the current analysis are marked by open circles and filled circles, respectively. To discriminate RGB and RC stars, we basically adopted results of Bedding et al. (2011) who differentiate them through the period spacing of mixed modes which are not fitted by the routine we used for the current analysis. However, for some stars observed by *K2* in which the mixed modes cannot be found, for example, since only a few number of peaks are recognized, we identify by ourselves the evolutionary status of stars as RGBs or RCs based on a

[1] https://keplergo.github.io/KeplerScienceWebsite/k2-fields.html

Table 1. Basic properties of the four star clusters being considered in the present analysis.

	NGC 2682	NGC 6819	NGC 1817	NGC 6811	References
$\tau_{\rm iso}$ (Gyr)	3.758 ± 0.242	2.630 ± 0.176	1.236 ± 0.048	1.007 ± 0.049	Dias et al. (2021)
$[{\rm Fe/H}]_{\rm iso}$	0.072 ± 0.052	0.093 ± 0.006	-0.100 ± 0.019	0.032 ± 0.015	Dias et al. (2021)
M ($M_\odot$)	2818	15136	2570	1288	Jadhav & Subramaniam (2021)
$\lvert Z\rvert$ (pc)	454.3	383.4	388.5	231.3	Cantat-Gaudin & Anders (2020)
ρ ($M_\odot/{\rm pc}^3$)	0.164	6.463	1.930	3.914	Kharchenko et al. (2013)
$r_{\rm core}/r_{\rm cluster}$	0.101 ± 0.001	0.214 ± 0.015	0.355 ± 0.088	0.423 ± 0.091	Kharchenko et al. (2013)
$r_{\rm tidal}/r_{\rm cluster}$	1.124 ± 0.116	1.617 ± 0.117	1.549 ± 0.338	1.583 ± 0.285	Kharchenko et al. (2013)
$M_{\rm RGB}$ ($M_\odot$)	1.128 ± 0.015	1.176 ± 0.019	1.226 ± 0.013	—	Anders et al. (2019)
$M_{\rm RC}$ ($M_\odot$)	1.233 ± 0.030	1.266 ± 0.015	1.374 ± 0.052	1.846 ± 0.041	Anders et al. (2019)

position in the CMD (Stello et al. 2016; Sandquist et al. 2020). In Table 1, we list up basic properties of the four star clusters being considered in this paper. To determine the age $\tau_{\rm iso}$ and metallicity $[{\rm Fe/H}]_{\rm iso}$ which is converted from the metallicity parameter Z in the isochrone fit, implementing the PAdova and TRieste Stellar Evolution Code (PARSEC; Bertelli et al. 2008; Bressan et al. 2012), isochrone fittings for the four open clusters are executed typical based on Gaia DR2 photometry data (Dias et al. 2021). The mass of the star cluster, vertical distance from the Galactic plane $|Z|$, and its mass density ρ are also provided. The core radius $r_{\rm core}$ and tidal radius $r_{\rm tidal}$ of the star cluster in King (1962) profile, extracted from the Milky Way Star Clusters Catalog (MWSC) (Kharchenko et al. 2013), are given in its cluster radius $r_{\rm cluster}$. For comparison, we also provide the averaged mass of individual RGB and RC stars used in this analysis, taken from the StarHorse catalog (Anders et al. 2019).

In retrieving the time series of the light curve of stars, it is necessary to identify cluster members with their KIC/EPIC Identification Numbers. For star clusters NGC 6819 and NGC 6811 in the *Kepler* field, we follow the membership determination strategy proposed by Cantat-Gaudin et al. (2018) where Unsupervised Photometric Membership Assignment in Stellar Clusters (UPMASK) is applied to the Gaia DR2 data. For the eight stars in NGC 6819, membership determinations are derived from other sources: KIC 5112558 (Hole et al. 2009), KIC 4937775, 5024582, 5112361 (Milliman et al. 2014), KIC 4936463, 5023889, 5024043, 5025472 (Poovelil et al. 2020). For the *K2* clusters NGC 2682 and NGC 1817, we rely on the following membership sources: NGC 2682 (Geller et al. 2015; Carrera et al. 2019) and NGC 1817 (Sandquist et al. 2020).

We download time series data from the Mikulski Archive for Space Telescopes (MAST)[2]. For *Kepler* data, we use the Pre-search Data Conditioning Simple Aperture Photometry (PDCSAP) flux. During Pre-search Data Conditioning (PDC), instrumental perturbations, such as, attitude tweaks and safe mode events, are corrected. For *K2* data, we use the dataset in which the noise induced by reaction wheel troubles is removed using the Self Flat-Fielding (SFF) method (Vanderburg & Johnson 2014). Having downloaded the light curve data, we organize the time series to reduce noise in the power spectrum. For example, we remove outliers and fill gaps with Gaussian random noise. We also get rid of long-term variations using the Savitzky-Golay high-pass filter (Savitzky & Golay 1964).

We compute the oscillation spectra of the 233 evolved stars with membership probabilities exceeding 70% using the Lomb-Scargle periodogram (Lomb 1976; Scargle 1982). We subsequently execute the Gaussian fit to the observed stellar power spectrum to determine the global seismic parameters. We presume that the obtained stellar power spectrum consists of the stellar oscillation power excess $P(\nu)$ centered at $\nu_{\rm max}$, background red-noise of the stellar power spectrum $B(\nu)$, and background white-noise W. The main signal $P(\nu)$ is described by the Gaussian envelope as

$$P(\nu) = H_{\rm Gauss} \exp\left[-\frac{(\nu - \nu_{\rm max})^2}{2\sigma_{\rm e}^2}\right], \qquad (6)$$

where $\delta\nu_{\rm env} = 2\sqrt{2\ln 2}\,\sigma_{\rm e}$ is the full-width at half-maximum (FWHM) of the mode envelope, and $H_{\rm Gauss}$ is the height of the power spectrum at $\nu_{\rm max}$. For the background red-noise of the acoustic power spectrum, we adopt the Karoff model with $n = 2$ (Karoff 2008; Mathur et al. 2011). To obtain the large separation frequency $\Delta\nu$, we calculate the 2D autocorrelation function of the stellar power spectrum (Roxburgh & Vorontsov 2006; Huber et al. 2009; Mosser & Appourchaux 2009; Viani et al. 2019). A series of autocorrelations are computed for a window of $2 \times$ FWHM (Mosser et al. 2010; Lund et al. 2017; Lightkurve Collaboration et al. 2018). To determine $\delta\nu_{02}$, we estimate the mode frequencies for $l = 0$ and $l = 2$ by Bayesian peak-bagging using Markov Chain Monte Carlo sampling (Appourchaux 2003; Nielsen et al. 2021).

For NGC 2682, we measure asteroseismic quantities for 19 giant stars observed during *K2* campaigns 5, 16, and 18 (cf. Stello et al. 2016). For NGC 6819, the asteroseismic quantities for 53 giant members are measured. We add into our dataset KIC 5112558 (Hole et al. 2009), KIC 4937775, 5024582, 5112361 (Milliman et al. 2014), KIC 4936463, 5023889, 5024043, 5025472 (Poovelil et al. 2020). For NGC 1817, asteroseismic quantities for 19 giant stars are measured. In the current study, NGC 6811 has the fewest stars, and thus, asteroseismic quantities can be reliably extracted for only seven giant stars.

[2] http://mast.stsci.edu/

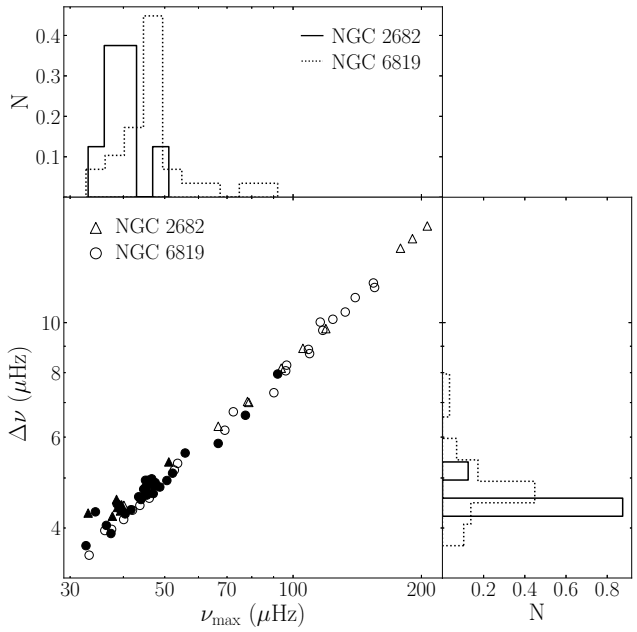

Figure 2. Relations between $\nu_{\rm max}$ and $\Delta\nu$ and number distributions N of RC stars. Triangles and solid lines represent NGC 2682, circles and dotted lines represent and NGC 6819. Open and filled symbols represent RGB and RC stars, respectively.

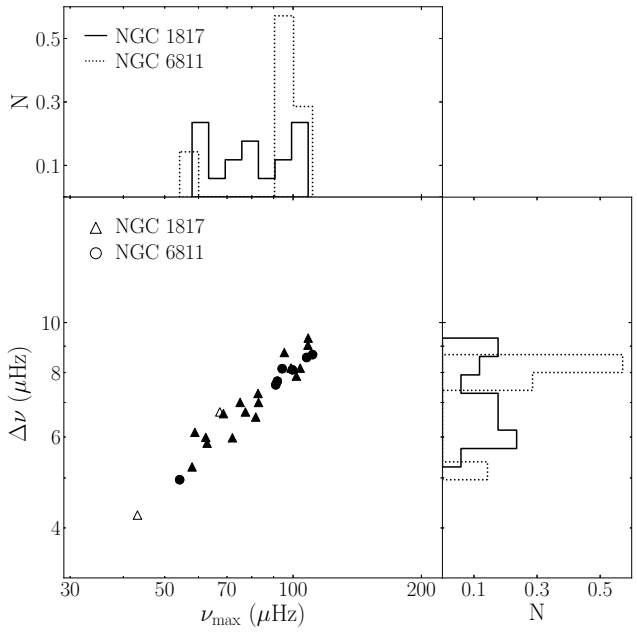

Figure 3. Similar to Figure 2, but showing results from NGC 1817 and NGC 6811.

3. Results

In Figure 2, we show the relation between $\nu_{\rm max}$ and $\Delta\nu$ resulting from 72 giant stars. Triangles and circles stand for NGC 2682 and NGC 6819, respectively, as denoted in the top left. Open and filled symbols represent RGB and RC stars, respectively, for all the remaining figures throughout the paper. It should be worthwhile to remind that the RGB stars are distributed in a broader range of $\nu_{\rm max}$ and $\Delta\nu$ compared with RC stars, in general, as evidenced by the wide distribution of RGB stars along the vertical axis of the Kiel diagram of a star cluster. Considering Equations (2) and (3), this fact implies that RGB stars may differ considerably in their density and surface gravity despite having similar masses. We also show the number distributions of RC stars along the $\nu_{\rm max}$ and $\Delta\nu$ axes, which are obtained by projecting to the corresponding axes, respectively. Solid and dotted lines represent NGC 2682 and NGC 6819, respectively. All the histograms produced in this paper are normalized such that the total area is equal to unity. In Figure 3, we show similar plots, but showing results for NGC 1817 and NGC 6811. Triangles and circles, as well as solid and dotted lines represent NGC 1817 and NGC 6811, respectively, as designated in the top left.

Table 2. Results of power law fit for $\Delta\nu = a\nu_{\rm max}^{b}$.

Clusters	State	a	b
NGC 2682	RGB	0.2151 ± 0.0035	0.8019 ± 0.0032
	RC	0.4699 ± 0.0646	0.6135 ± 0.0372
NGC 6819	RGB	0.2394 ± 0.0032	0.7742 ± 0.0029
	RC	0.3504 ± 0.0063	0.6820 ± 0.0046
NGC 1817	RGB	—	—
	RC	0.2672 ± 0.0200	0.7464 ± 0.0168
NGC 6811	RGB	—	—
	RC	0.2347 ± 0.0225	0.7705 ± 0.0210

Bearing in mind that averaged masses of RGB, and RC stars in NGC 2682 and NGC 6819 are 1.128 and 1.176 $M_\odot$, and 1.233 and 1.266 $M_\odot$, respectively, the relation between $\Delta\nu$ and $\nu_{\rm max}$ should be expected to follow a single relation as a power law $\Delta\nu \approx a\nu_{\rm max}^{b}$ without significant mass dependency (Hekker et al. 2009; Huber et al. 2009; Stello et al. 2009; Bedding et al. 2010; Huber et al. 2010; Mosser et al. 2010, 2012; Arentoft et al. 2017; Handberg et al. 2017; Yu et al. 2018; Li et al. 2020; Howell et al. 2022). In other words, results from the older cluster are not supposed to lie above those from the younger cluster. However, the best fits obtained from RGB stars in NGC 2682 and NGC 6819 with the least squares method are $\Delta\nu \propto \nu_{\rm max}^{0.8019\pm0.0032}$ and $\propto \nu_{\rm max}^{0.7742\pm0.0029}$, respectively. As for RC stars, the best fits from NGC 2682 and NGC 6819 with the least squares method are $\Delta\nu \propto \nu_{\rm max}^{0.6135\pm0.0372}$ and $\propto \nu_{\rm max}^{0.6820\pm0.0046}$, respectively. From Figure 3, the best fits obtained from RC stars in NGC 1817 and NGC 6811 with the least squares method are $\Delta\nu \propto \nu_{\rm max}^{0.7464\pm0.0168}$ and $\propto \nu_{\rm max}^{0.7705\pm0.0210}$, respectively. Results are listed in Table 2. The typical standard error of $\nu_{\rm max}$ in the plot is 0.11 μHz and the typical fractional uncertainty of $\Delta\nu$ is 0.4%.

We note that, according to the ratios of $r_{\rm core}$ and $r_{\rm tidal}$ to $r_{\rm cluster}$ listed in Table 1, NGC 2682 and NGC 1817 are less dense on average and yet more concentrated than NGC 6819 and NGC 6811, respectively. NGC 2682 and NGC 1817 are farther away from the Galactic disk than NGC 6819 and NGC 6811, respectively. Thus, it is concluded that for RGB stars the slope from the more concentrated star-cluster is steeper than that for the less concentrated star-cluster. As for

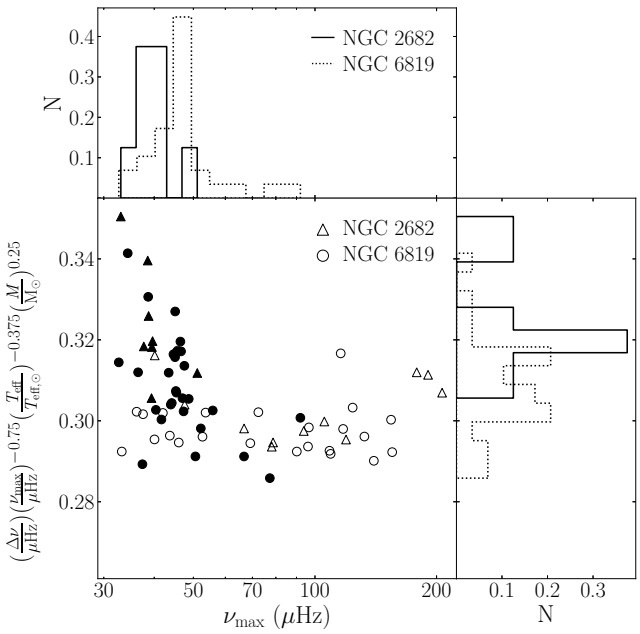

Figure 4. Similar to Figure 2, but showing results for $\Delta\nu\nu_{\rm max}^{-0.75}T_{\rm eff}^{-0.375}M^{0.25}$.

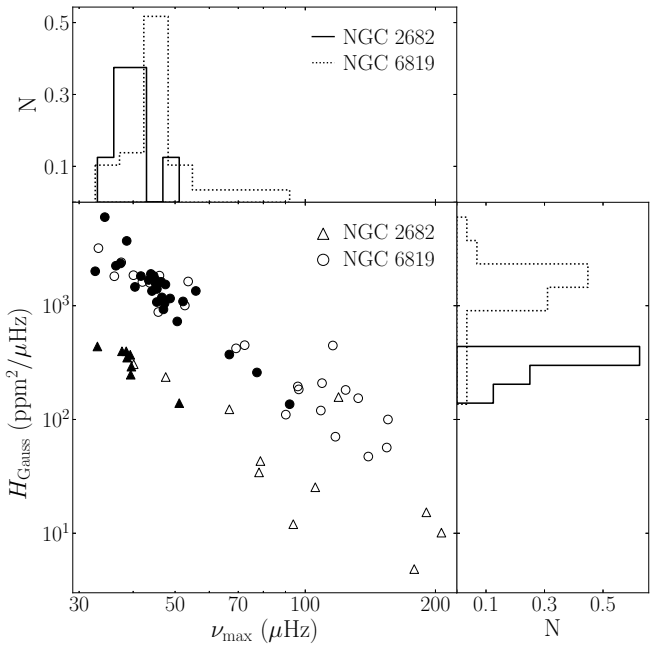

Figure 6. Similar to Figure 2, but showing results for $H_{\rm Gauss}$.

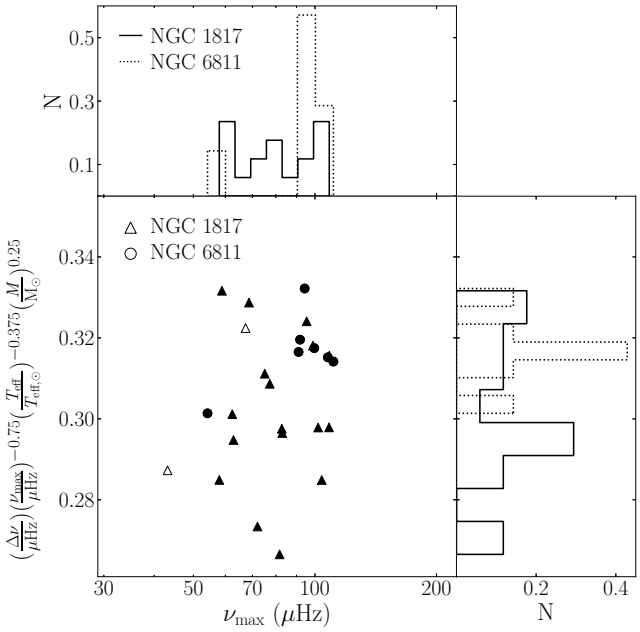

Figure 5. Similar to Figure 4, but showing results from NGC 1817 and NGC 6811.

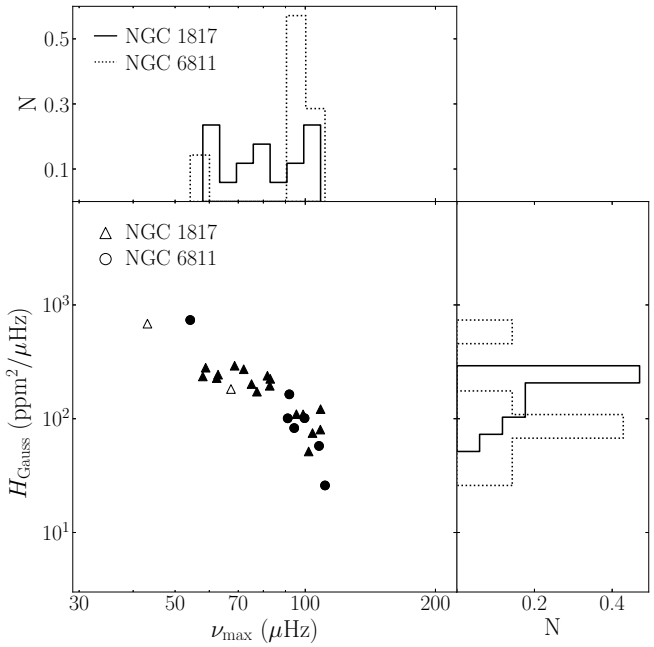

Figure 7. Similar to Figure 6, but showing results from NGC 1817 and NGC 6811.

RC stars, the slope from the more concentrated star-clusters, NGC 2682 and NGC 1817, is in common less steep compared with those for the less concentrated star-clusters, NGC 6819 and NGC 6811.

In Figures 4 and 5, to ensure that the mass effect in the obtained relation between $\nu_{\rm max}$ and $\Delta\nu$ in our analysis using cluster-pairs of similar age is negligible, we show the relation between $\nu_{\rm max}$ and $\Delta\nu\nu_{\rm max}^{-0.75}T_{\rm eff}^{-0.375}M^{0.25}$ resulting from the pair of NGC 2682 and NGC 6819, and that of NGC 1817 and NGC 6811, respectively. Triangles and circles represent the star clusters as designated. As expected, this treatment removes the dependence on all the parameters. Nevertheless, it is interesting to note that RGB and RC stars seem to be distributed separately in different domains of the plot. That is, RGB stars are spread horizontally, while the distribution of RC stars shows a diagonal structure. What it implies is that the mass effect for RGB stars is well removed through the scaling relation, but not for RC stars. The diagonal structure of RC stars

Table 3. Results of power law fit for $H_{\rm Gauss} = a\nu_{\rm max}^{b}$.

Clusters	State	a	b
NGC 2682	RGB	$(8.29 \pm 4.56) \times 10^{5}$	-2.1358 ± 0.1428
	RC	$(1.23 \pm 0.96) \times 10^{6}$	-2.2461 ± 0.2145
NGC 6819	RGB	$(8.14 \pm 1.47) \times 10^{6}$	-2.2655 ± 0.0491
	RC	$(7.98 \pm 2.86) \times 10^{7}$	-2.8503 ± 0.0971
NGC 1817	RGB	—	—
	RC	$(1.40 \pm 0.44) \times 10^{5}$	-1.5223 ± 0.0726
NGC 6811	RGB	—	—
	RC	$(1.04 \pm 0.38) \times 10^{9}$	-3.5456 ± 0.0916

which is widely known seems to be due to structural properties of the stars in the different stages of stellar evolution rather than environmental influences. The slopes obtained from RGB stars in NGC 2682 and NGC 6819 with the least squares method are 0.0065 ± 0.0158 and -0.0071 ± 0.0094, respectively. For RC stars in NGC 2682 and NGC 6819, the slopes are -0.2539 ± 0.1204 and -0.0987 ± 0.0314, respectively. The slopes for RC stars in NGC 1817 and NGC 6811 are determined to be 0.0002 ± 0.0731 and 0.0715 ± 0.0439, respectively.

In Figures 6 and 7, we show the plot of $H_{\rm Gauss}$ against $\nu_{\rm max}$ for the pair of NGC 2682 and NGC 6819, and that of NGC 1817 and NGC 6811, respectively. Triangles and circles represent the star clusters as designated. The values of $H_{\rm Gauss}$ typically decrease with increasing $\nu_{\rm max}$ (Mosser et al. 2012, 2013). The slopes resulting from RGB stars in NGC 2682 and NGC 6819 are -2.1358 ± 0.1428, -2.2655 ± 0.0491, respectively, and those from RC stars -2.2461 ± 0.2145, -2.8503 ± 0.0971, respectively. For RC stars in NGC 1817 and NGC 6811, the obtained slopes are -1.5223 ± 0.0726 and -3.5456 ± 0.0916, respectively. Results are listed in Table 3, and the typical standard error of $H_{\rm Gauss}$ in the plot is 2.27 ppm$^2/\mu$Hz. Hence, it is concluded that for both RGB and RC stars the slopes from the more concentrated star-clusters are all less steep compared with those for the less concentrated star-clusters.

In Figures 8 and 9, we show the plot of $\delta\nu_{\rm env}$ as a function of $\nu_{\rm max}$ from the pair of NGC 2682 and NGC 6819, and that of NGC 1817 and NGC 6811, respectively. Triangles and circles represent star clusters as designated in the top left. In general, the width of the Gaussian envelope increases with increasing $\nu_{\rm max}$ (Kim & Chang 2021). The slopes resulting from RGB stars in NGC 2682 and NGC 6819 are 0.7217 ± 0.0523, 0.8673 ± 0.0171, respectively, and those from RC stars are 1.3209 ± 0.2566, 1.1765 ± 0.0097, respectively. For RC stars in NGC 1817 and NGC 6811, the obtained slopes are 0.8628 ± 0.0794 and 0.7886 ± 0.2114, respectively. Results are listed in Table 4, and the typical standard error of $\delta\nu_{\rm env}$ in the plot is 0.46 μHz. Therefore, it is concluded that for RGB stars the slope from the more concentrated star-cluster is less steep than that for the less concentrated star-cluster. As for RC stars, the slopes from the more concentrated star-clusters are in common steeper compared with those for the less concentrated star-clusters.

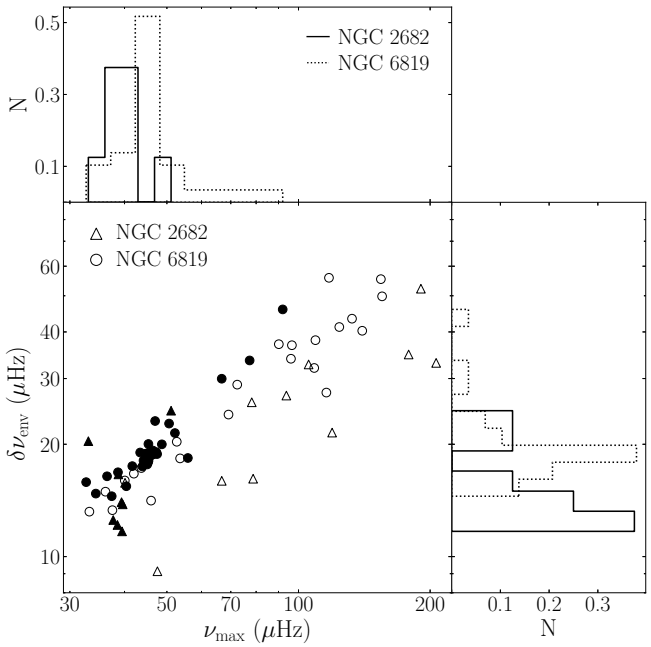

Figure 8. Similar to Figure 2, but showing results for $\delta\nu_{\rm env}$.

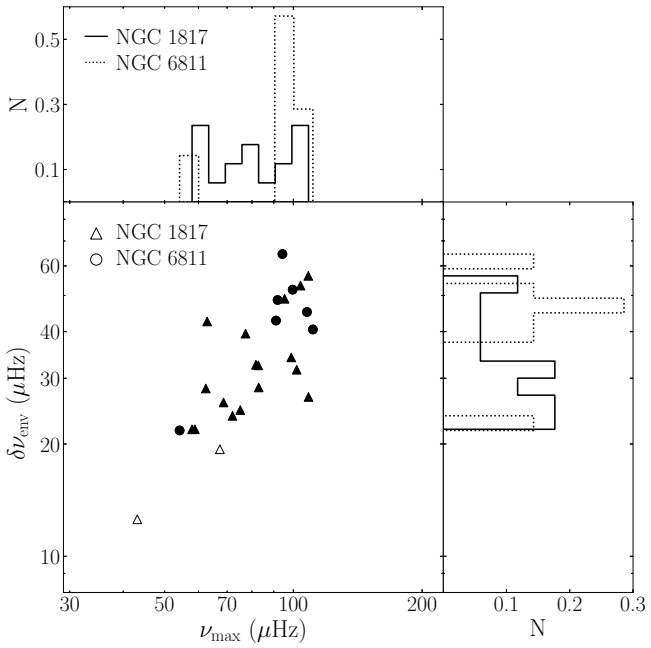

Figure 9. Similar to Figure 8, but showing results from NGC 1817 and NGC 6811.

Table 4. Results of power law fit for $\delta\nu_{\rm env} = a\nu_{\rm max}^{b}$.

Clusters	State	a	b
NGC 2682	RGB	0.8953 ± 0.2311	0.7217 ± 0.0523
	RC	0.1208 ± 0.1152	1.3209 ± 0.2566
NGC 6819	RGB	0.6421 ± 0.0516	0.8673 ± 0.0171
	RC	0.2119 ± 0.0082	1.1765 ± 0.0097
NGC 1817	RGB	—	—
	RC	0.7514 ± 0.2663	0.8628 ± 0.0794
NGC 6811	RGB	—	—
	RC	1.2714 ± 1.2284	0.7886 ± 0.2114

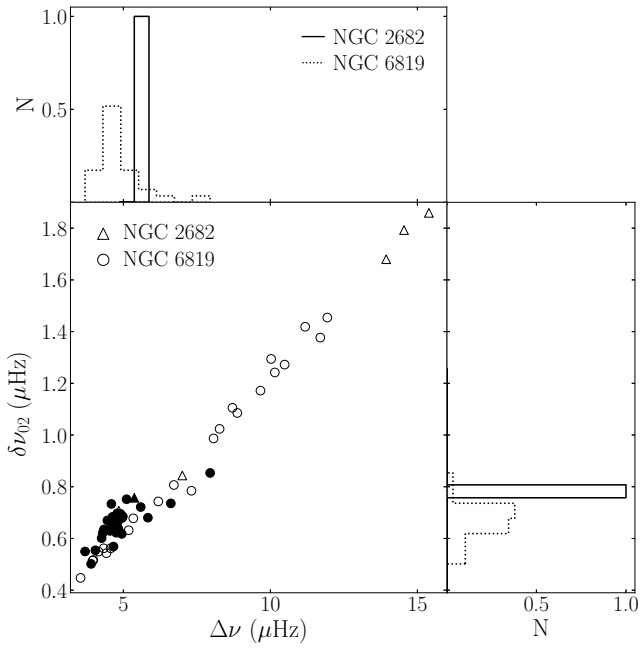

Figure 10. Similar to Figure 2, but showing the relation of $\delta\nu_{02}$ with $\Delta\nu$.

In Figure 10, we show the relation between $\delta\nu_{02}$ and $\Delta\nu$, so-called C-D diagram (Christensen-Dalsgaard 1988), in which stars evolve from the top-right to the bottom-left following well separated evolutionary tracks with different masses during the main sequence stage. However, the tracks converge during the subgiant and red giant stages (Monteiro et al. 2002; Otí Floranes et al. 2005; Gai et al. 2009; Bedding et al. 2010; Huber et al. 2010; Montalbán et al. 2010; White et al. 2011; Corsaro et al. 2012; Handberg et al. 2017; Li et al. 2020; Dréau et al. 2021). Because of this nature of the convergence, $\delta\nu_{02}$ must be precisely measured for giant stars. Since it is necessary to have clearly identifiable $l = 0$ and $l = 2$ modes to measure $\delta\nu_{02}$, high signal-to-noise ratios are required. For this reason, we can only afford to accurately measure the mean small frequency separation $\delta\nu_{02}$ for the pair of NGC 2682 and NGC 6819. For RGB stars in NGC 2682 and NGC 6819, the obtained slopes are 0.1139 ± 0.0023 and 0.1193 ± 0.0006, respectively. Results are listed in Table 5, and the typical standard error of $\delta\nu_{02}$ in the plot is 0.14 μHz. It is concluded, therefore, that the slopes from two star clusters remain comparable for RGB stars.

To statistically assess whether the number distributions of giant stars resulting from the two pairs of star clusters are compatible with each other we further perform the Kolmogorov-Smirnov (K-S) test. Applying the K-S tests to the number distributions of $\Delta\nu$ and $\nu_{\rm max}$ from RC stars in NGC 2682 and NGC 6819 return all the p-values less than 0.01, rejecting the null hypothesis that the two samples of $\Delta\nu$ and $\nu_{\rm max}$ from NGC 2682 and NGC 6819 are drawn from the same distribution. In contrast, as for RGB stars in NGC 2682 and NGC 6819, the K-S statistic D and p-value signify that $\Delta\nu$ and $\nu_{\rm max}$ seemingly share the same distributions. In the meantime, the K-S test on the distributions of $\Delta\nu$ and $\nu_{\rm max}$ from RC stars in NGC 1817 and NGC 6811 returns statistic D and p-value which marginally indicate that the distributions of NGC 1817 are different from those of NGC 6811. K-S tests on the distributions of $\Delta\nu\nu_{\rm max}^{-0.75}T_{\rm eff}^{-0.375}M^{0.25}$ from RC stars in the pairs of NGC 2682 and NGC 6819, and of NGC 1817 and NGC 6811 yield the results implying that they are all different distributions. K-S tests on the distributions of $H_{\rm Gauss}$ from RGB and RC stars of NGC 2682 and NGC 6819 yield the results implying that they are all different distributions. For NGC 1817 and NGC 6811, K-S tests on the distributions of $H_{\rm Gauss}$ from RC stars alone indicate that the distributions are different each other. K-S tests on the distributions of $\delta\nu_{\rm env}$ from RC stars in the pairs of NGC 2682 and NGC 6819, and of NGC 1817 and NGC 6811 yield the results implying that they are all different distributions. For NGC 2682 and NGC 6819, the K-S test on the distributions of $\delta\nu_{02}$ from RGB stars implies that the distributions are different each other.

Table 5. Results of linear fit for $\delta\nu_{02} = a\Delta\nu + b$.

Clusters	State	a	b
NGC 2682	RGB	0.1139 ± 0.0023	0.1074 ± 0.0270
	RC	—	—
NGC 6819	RGB	0.1193 ± 0.0006	0.0304 ± 0.0045
	RC	0.0680 ± 0.0018	0.3265 ± 0.0090

4. Summary and Conclusions

Individual objects in the Universe interact with their environment during their lifetime since their formation. In particular, stellar properties seem to be modified as a result of encounters and collisions with neighboring stars in dense regions such as star cluster. In this study, we attempt to address the issue whether observed stellar oscillations can be influenced by these environments, motivated by the discovery of unusual pulsators in star clusters. To this end, we analyze asteroseismic data from evolved stars in star clusters observed by *Kepler*/*K2*, and carefully compare statistical properties of $\Delta\nu$, $\nu_{\rm max}$, $H_{\rm Gauss}$, $\delta\nu_{\rm env}$, and $\delta\nu_{02}$. Specifically, we examine if RGB and RC stars in the two pairs of star clusters, NGC 2682 - NGC 6819 and NGC 1817 - NGC 6811, come to the consistent results.

Our main findings are as follows:

(1) As for the relation between $\nu_{\rm max}$ and $\Delta\nu$, the slope from RGB stars in the more concentrated star cluster NGC 2682 is steeper than that for the less concentrated star cluster NGC 6819. The slopes from RC stars in the more concentrated star-clusters, NGC 2682 and NGC 1817, are in common less steep.

(2) According to the plot of $H_{\rm Gauss}$ against $\nu_{\rm max}$, the slopes from both RGB and RC stars in the more concentrated star-clusters, NGC 2682 and NGC 1817, are all less steep compared with those for the less concentrated star-clusters, NGC 6819 and NGC 6811.

(3) The slope of $\delta\nu_{\rm env}$ as a function of $\nu_{\rm max}$ from RGB stars in the more concentrated star-cluster NGC 2682 is less steep than that for the less concentrated star-cluster NGC 6819

for RGB stars. For RC stars, the slopes from the more concentrated star-clusters, NGC 2682 and NGC 1817, are in common steeper.

(4) In the relation between $\delta\nu_{02}$ and $\Delta\nu$ obtained from RGB stars, the slopes resulting from NGC 2682 and NGC 6819 are not dissimilar.

(5) The K-S tests of RC stars in the pair of NGC 2682 and NGC 6819, and that of NGC 1817 and NGC 6811 yield the outcomes implying that all the seismic quantities considered in this work are likely drawn from different distributions. For RGB stars, K-S tests on $H_{\rm Gauss}$ and $\delta\nu_{02}$ with a pair of NGC 2682 and NGC 6819 imply that the distributions are different each other. In contrast, K-S tests on the distributions of $\Delta\nu$, $\nu_{\rm max}$, and $\delta\nu_{\rm env}$ for RGB stars in NGC 2682 and NGC 6819 yield results indicating that they seemingly share the same distributions.

Changes in internal dynamics and structures induced either by mixing processes leading to chemical modifications or tidal force-induced swelling within dense environments of star clusters, can be revealed as asteroseismology is a sensitive tool for studying acoustic oscillations trapped in their own resonant cavity. According to what we have found in this paper, RC stars appear more sensitive to star clusters compared with RGB stars. We conclude, therefore, that the properties of star cluster should be taken into account in the interpretation of asteroseismic data obtained from stars in star clusters, particularly when the dependence of parameters other than the primary factor, i.e., mass, is considered to precisely estimate physical quantities.

Acknowledgments

The authors thank the anonymous referees for critical comments and helpful suggestions. This study was funded by Basic Science Research Program Through the National Research Foundation (NRF) of Korea funded by the Ministry of Science, ICT and future Planning (2018R1A6A1A06024970).

References

Abedigamba, O. P., Balona, L. A., & Medupe, R. 2016, New A, 46, 90
Anders, F., Chiappini, C., Rodrigues, T. S., et al. 2017, A&A, 597, A30
Anders, F., Khalatyan, A., Chiappini, C., et al. 2019, A&A, 628, A94
Appourchaux, T. 2003, Ap&SS, 284, 109
Arentoft, T., Brogaard, K., Jessen-Hansen, J., et al. 2017, ApJ, 838, 115
Baglin, A., Auvergne, M., Barge, P., et al. 2006, in ESA Spec. Publ., Vol. 1306, The CoRoT Mission Pre-Launch Status - Stellar Seismology and Planet Finding, ed. M. Fridlund, A. Baglin, J. Lochard, & L. Conroy, 33
Basu, S., Grundahl, F., Stello, D., et al. 2011, ApJ, 729, L10
Bedding, T. R., Huber, D., Stello, D., et al. 2010, ApJ, 713, L176
Bedding, T. R., Mosser, B., Huber, D., et al. 2011, Nature, 471, 608
Belkacem, K., Goupil, M. J., Dupret, M. A., et al. 2011, A&A, 530, A142
Bellinger, E. P. 2020, MNRAS, 492, L50
Bertelli, G., Girardi, L., Marigo, P., & Nasi, E. 2008, A&A, 484, 815
Borucki, W. J., Koch, D., Basri, G., et al. 2010, Science, 327, 977
Bressan, A., Marigo, P., Girardi, L., et al. 2012, MNRAS, 427, 127
Brogaard, K., Hansen, C. J., Miglio, A., et al. 2018, MNRAS, 476, 3729
Brown, T. M., Gilliland, R. L., Noyes, R. W., & Ramsey, L. W. 1991, ApJ, 368, 599
Cantat-Gaudin, T., & Anders, F. 2020, A&A, 633, A99
Cantat-Gaudin, T., Jordi, C., Vallenari, A., et al. 2018, A&A, 618, A93
Carrera, R., Pasquato, M., Vallenari, A., et al. 2019, A&A, 627, A119
Carroll, B. W., & Ostlie, D. A. 2017, An introduction to modern astrophysics, 2nd edn. (Cambridge: Cambridge University Press)
Chaplin, W. J., & Miglio, A. 2013, ARA&A, 51, 353
Chaplin, W. J., Basu, S., Huber, D., et al. 2014, ApJS, 210, 1
Christensen-Dalsgaard, J. 1988, in IAU Symposium, Vol. 123, Advances in Helio- and Asteroseismology, ed. J. Christensen-Dalsgaard & S. Frandsen, 295
Coelho, H. R., Chaplin, W. J., Basu, S., et al. 2015, MNRAS, 451, 3011
Corsaro, E., Stello, D., Huber, D., et al. 2012, ApJ, 757, 190
Corsaro, E., Mathur, S., García, R. A., et al. 2017, A&A, 605, A3
Dias, W. S., Monteiro, H., Moitinho, A., et al. 2021, MNRAS, 504, 356
Dréau, G., Mosser, B., Lebreton, Y., Gehan, C., & Kallinger, T. 2021, A&A, 650, A115
Gai, N., Bi, S. L., Tang, Y. K., & Li, L. H. 2009, A&A, 508, 849
Geller, A. M., Latham, D. W., & Mathieu, R. D. 2015, AJ, 150, 97
Gough, D. O. 1986, in Hydrodynamic and Magnetodynamic Problems in the Sun and Stars, ed. Y. Osaki, 117
Handberg, R., Brogaard, K., Miglio, A., et al. 2017, MNRAS, 472, 979
Harvey, J. 1985, in ESA Spec. Publ., Vol. 235, Future Missions in Solar, Heliospheric & Space Plasma Physics, ed. E. Rolfe & B. Battrick, 199
Harvey, J. W., Duvall, T. L., J., Jefferies, S. M., & Pomerantz, M. A. 1993, in ASP Conf. Ser., Vol. 42, GONG 1992. Seismic Investigation of the Sun and Stars, ed. T. M. Brown, 111
Hekker, S., Kallinger, T., Baudin, F., et al. 2009, A&A, 506, 465
Hekker, S., Basu, S., Stello, D., et al. 2011, A&A, 530, A100
Hole, K. T., Geller, A. M., Mathieu, R. D., et al. 2009, AJ, 138, 159
Howell, M., Campbell, S. W., Stello, D., & De Silva, G. M. 2022, MNRAS, 515, 3184
Howell, S. B., Sobeck, C., Haas, M., et al. 2014, PASP, 126, 398
Huber, D., Stello, D., Bedding, T. R., et al. 2009, Commun. Asteroseismol., 160, 74
Huber, D., Bedding, T. R., Stello, D., et al. 2010, ApJ, 723, 1607
Iben, Icko, J. 1967, ARA&A, 5, 571
Jadhav, V. V., & Subramaniam, A. 2021, MNRAS, 507, 1699
Kallinger, T., Beck, P. G., Stello, D., & Garcia, R. A. 2018, A&A, 616, A104
Karoff, C. 2008, PhD thesis, Aarhus University, Denmark
Kharchenko, N. V., Piskunov, A. E., Schilbach, E., Röser, S., & Scholz, R. D. 2013, A&A, 558, A53
Kim, K.-B., & Chang, H.-Y. 2021, New A, 84, 101522
King, I. 1962, AJ, 67, 471
Kjeldsen, H., & Bedding, T. R. 1995, A&A, 293, 87
Koch, D. G., Borucki, W. J., Basri, G., et al. 2010, ApJ, 713, L79
Li, T., Li, Y., Bi, S., et al. 2022, ApJ, 927, 167
Li, Y., Bedding, T. R., Li, T., et al. 2020, MNRAS, 495, 2363

Lightkurve Collaboration, Cardoso, J. V. d. M., Hedges, C., et al. 2018, Astrophys. Source Code Libr., ascl:1812.013
Lomb, N. R. 1976, Ap&SS, 39, 447
Lund, M. N., Silva Aguirre, V., Davies, G. R., et al. 2017, ApJ, 835, 172
Mathur, S., Hekker, S., Trampedach, R., et al. 2011, ApJ, 741, 119
Michel, E., Baglin, A., Auvergne, M., et al. 2008, Science, 322, 558
Miglio, A., Brogaard, K., Stello, D., et al. 2012, MNRAS, 419, 2077
Miglio, A., Chiappini, C., Morel, T., et al. 2013, MNRAS, 429, 423
Milliman, K. E., Mathieu, R. D., Geller, A. M., et al. 2014, AJ, 148, 38
Montalbán, J., Miglio, A., Noels, A., Scuflaire, R., & Ventura, P. 2010, ApJ, 721, L182
Monteiro, M. J. P. F. G., Christensen-Dalsgaard, J., & Thompson, M. J. 2002, in ESA Spec. Publ., Vol. 485, Stellar Structure and Habitable Planet Finding, ed. B. Battrick, F. Favata, I. W. Roxburgh, & D. Galadi, 291
Mosser, B., & Appourchaux, T. 2009, A&A, 508, 877
Mosser, B., Belkacem, K., Goupil, M. J., et al. 2010, A&A, 517, A22
Mosser, B., Elsworth, Y., Hekker, S., et al. 2012, A&A, 537, A30
Mosser, B., Dziembowski, W. A., Belkacem, K., et al. 2013, A&A, 559, A137
Mowlavi, N., Saesen, S., Semaan, T., et al. 2016, A&A, 595, L1
Nielsen, M. B., Davies, G. R., Ball, W. H., et al. 2021, AJ, 161, 62
Otí Floranes, H., Christensen-Dalsgaard, J., & Thompson, M. J. 2005, MNRAS, 356, 671
Pinsonneault, M., Elsworth, Y., Silva Aguirre, V., et al. 2018, in AAS Meet. Abs., Vol. 231, 450.13
Poovelil, V. J., Zasowski, G., Hasselquist, S., et al. 2020, ApJ, 903, 55
Ricker, G. R., Winn, J. N., Vanderspek, R., et al. 2015, J. Astron. Telesc. Instrum. Syst., 1, 014003
Roxburgh, I. W., & Vorontsov, S. V. 2006, MNRAS, 369, 1491
Sackmann, I. J., Boothroyd, A. I., & Kraemer, K. E. 1993, ApJ, 418, 457
Sandquist, E. L., Stello, D., Arentoft, T., et al. 2020, AJ, 159, 96
Savitzky, A., & Golay, M. J. E. 1964, Anal. Chem., 36, 1627
Scargle, J. D. 1982, ApJ, 263, 835
Schröder, K. P., & Smith, R. C. 2008, MNRAS, 386, 155
Sharina, M. E., Shimansky, V. V., & Khamidullina, D. A. 2018, Astrophys. Bull., 73, 318
Sharma, S., Stello, D., Bland-Hawthorn, J., Huber, D., & Bedding, T. R. 2016, ApJ, 822, 15
Silva Aguirre, V., Chaplin, W. J., Ballot, J., et al. 2011, ApJ, 740, L2
Silva Aguirre, V., Bojsen-Hansen, M., Slumstrup, D., et al. 2018, MNRAS, 475, 5487
Stello, D., Chaplin, W. J., Basu, S., Elsworth, Y., & Bedding, T. R. 2009, MNRAS, 400, L80
Stello, D., Huber, D., Kallinger, T., et al. 2011, ApJ, 737, L10
Stello, D., Vanderburg, A., Casagrande, L., et al. 2016, ApJ, 832, 133
Tassoul, M. 1980, ApJS, 43, 469
Vanderburg, A., & Johnson, J. A. 2014, PASP, 126, 948
Viani, L. S., Basu, S., Corsaro, E., Ball, W. H., & Chaplin, W. J. 2019, ApJ, 879, 33
Walker, G., Matthews, J., Kuschnig, R., et al. 2003, PASP, 115, 1023
White, T. R., Bedding, T. R., Stello, D., et al. 2011, ApJ, 743, 161
Yu, J., Huber, D., Bedding, T. R., et al. 2018, ApJS, 236, 42
Zhou, J., Bi, S., Yu, J., et al. 2024a, ApJS, 271, 17
Zhou, Y., Christensen-Dalsgaard, J., Asplund, M., et al. 2024b, ApJ, 962, 118